A Less-Disturbed Ecological Driving Strategy for Connected and Automated Vehicles

Jinsong Yang, Dezong Zhao, *Senior Member, IEEE*, Jingjing Jiang, *Member, IEEE*, Jianglin Lan, Byron Mason, Daxin Tian, *Senior Member, IEEE*, and Liang Li, *Senior Member, IEEE*

***Abstract*—This paper proposes a less-disturbed ecological driving strategy for connected and automated vehicles (CAVs). The proposed strategy integrates the offline planning and the online tracking. In offline planning, an energy efficient reference speed is created based on traffic information (such as the average traffic speed) and characteristics of the vehicle (such as the engine efficiency map) via dynamic programming. The consideration of average traffic speed in speed planning avoids selfish optimisations. In online tracking, model predictive control is employed to update the vehicle speed in real-time to track the reference speed. A key challenge in applying ecological driving strategies in real driving is that the vehicle has to consider other traffic participants when tracking the reference speed. Therefore, this paper combines both longitudinal control and lateral control to achieve better speed tracking by overtaking the preceding vehicle when necessary. The proposed less-disturbed ecological driving strategy has been evaluated in simulations in both single road segment scenario and real traffic environment. Comparisons of the proposed method with benchmark strategies and human drivers are made. The results demonstrate that the proposed less-disturbed ecological driving strategy is more effective in energy saving. Compared to human drivers, the less-disturbed eco-driving strategy improves the fuel efficiency of CAVs by 4.53%.**

***Index Terms*—Dynamic programming, less-disturbed ecological driving, local adaptation, speed optimisation.**

NOMENCLATURE

$\dot{m}_f$	Engine fuel mass flow rate
T_ω	Output torque of the internal combustion engine
ω_e	Crankshaft rotational speed
$r_{\rm gb}$	Ratio of each gear including the final drive ratio
$\omega_{\rm wheel}$	Wheel rotational speed
Δs	Longitudinal distance step size
N	Total number of distance steps in distance-based offline planning
N_t	Total number of time steps in online tracking
S	Total route distance
P	Prediction horizon in model predictive control
$T_{\rm brk}$	Braking torque
m	Vehicle mass
r_w	Vehicle wheel radius
θ	Road grade
ρ	Air density
A	Front cross-sectional area
C_d	Air drag coefficient
$C_{\rm rr}$	Rolling resistance coefficient
v_x, v_y	Vehicle longitudinal and lateral velocities in the body framework
X_c, Y_c	Longitudinal and lateral positions of the vehicle in a global coordinate
ω_r, ψ	Yaw rate and yaw angle of the controlled CAV
C_f, C_r	Cornering stiffness of front and rear tyres
l_f, l_r	Distances from the front and rear axles to the centre of gravity
m	Vehicle mass
δ_f	Front wheel angle
a_x, a_y	Longitudinal and lateral accelerations in the body framework
I	Number of the road segments along the route
$V^i_{\rm avg}$	Average speed of the $i^{\rm th}$ road segment
$N_{\rm gear}$	Number of the selected gear
k	Number of steps
v^n_x, X^n	Longitudinal speed and position of the preceding vehicle n
T_s	Sampling time
$v_{\rm ref}$	Reference speed obtained in offline planning
t_s	Motion decision desired time between the preceding vehicle and the controlled CAV
Δv	Difference in velocity between the controlled CAV and the objective vehicle on the target lane
t_c	Desired time of lane change
δ_{t_x}	Longitudinal safety time between the preceding vehicle and the controlled CAV

Manuscript received 7 September 2020; revised 29 April 2021; accepted 29 August 2021. Date of publication 14 September 2021; date of current version 23 January 2023. This work was supported in part by the EPSRC Innovation Fellowship of the Engineering and Physical Sciences Research Council of U.K. under Grant EP/S001956/1, in part by Royal Society-Newton Advanced Fellowship under Grant NAF\R1\201213, and in part by the State Key Laboratory of Automotive Safety and Energy at Tsinghua University under Project KF2009. *(Corresponding author: Dezong Zhao.)*

Jinsong Yang is with the James Watt School of Engineering, University of Glasgow, Glasgow G12 8QQ, U.K. (e-mail: 2618741y@student.gla.ac.uk).

Dezong Zhao is with the James Watt School of Engineering, University of Glasgow, Glasgow G12 8QQ, U.K., and also with the State Key Laboratory of Automotive Safety and Energy, Tsinghua University, Beijing 100084, China (e-mail: Dezong.zhao@glasgow.ac.uk).

Jingjing Jiang and Byron Mason are with the Department of Aeronautical and Automotive Engineering, Loughborough University, Loughborough LE11 3TU, U.K. (e-mail: J.Jiang2@lboro.ac.uk; b.mason2@lboro.ac.uk).

Jianglin Lan is with the Department of Computing, Imperial College London, London SW7 2AZ, U.K. (e-mail: j.lan@imperial.ac.uk).

Daxin Tian is with the School of Transportation Science and Engineering, Beihang University, Beijing 100191, China (e-mail: dtian@buaa.edu.cn).

Liang Li is with the State Key Laboratory of Automotive Safety and Energy, Tsinghua University, Beijing 100084, China (e-mail: liangl@tsinghua.edu.cn).

Color versions of one or more figures in this article are available at https://doi.org/10.1109/TIV.2021.3112499.

Digital Object Identifier 10.1109/TIV.2021.3112499

This work is licensed under a Creative Commons Attribution 4.0 License. For more information, see https://creativecommons.org/licenses/by/4.0/

d_{safety_x}	Safety distance to avoid the collisions at low vehicle speeds
Y	Constraints of the CAV lateral position
r_y	Reference lateral position
l	Lane width
t	Travel time

I. Introduction

DUE to the shortage of fossil fuels and rising globally environmental concerns, improving the energy efficiency of transportation systems has become essential over the years. The ecological (eco)-driving strategies can assist vehicles to operate in fuel efficient conditions by running under optimal speed profiles. It is generally accepted that eco-driving strategies can substantially improve the efficiency of vehicles [1]. Some studies indicated that eco-driving strategies can improve vehicle fuel economy up to 25% [2]. Connected and automated vehicles (CAVs) have access to more and further road information than conventional vehicles using advanced technologies, such as vehicle-to-vehicle (V2V) communications, vehicle-to-infrastructure (V2I) communications and intelligent transportation systems (ITS) [3], [4]. These technologies enable CAVs to acquire the future route's traffic information, in terms of traffic flow rate, traffic density and traffic signal timing. The traffic density and traffic flow rate information can be utilised to provide the average speed in optimising the vehicle's future speed. The most significant benefit of considering the average speed of an area is that it considers the real traffic condition and avoids selfish optimisations which can create traffic waves and reduces capacity.

Based on the above techniques, some eco-driving strategies of CAVs have been investigated. Meanwhile, eco-driving strategies of CAVs can also be applied to conventional vehicles as speed advisors. An energy saving method called the eco-approach and departure (EAD) strategy is developed for vehicles that approach the signalised intersection [5]–[7]. The EAD strategy reduces or avoids the vehicle engine idling at the intersections. Meanwhile, some authors [8]–[10] consider the impacts from vehicle that queues at the signalised intersection, while vehicle queuing can be transformed into a delay. In the EAD method, the critical information is the signal phase and timing (SPaT) information from ITS and V2I. The SPaT information is the real-time traffic signal data on the route [11] of CAVs, which can help the eco-driving strategies to find the time slot passing the intersection. The EAD strategy divides vehicles motion into four possible cases when CAVs approach the intersection: cruise, speed-up, full stop and coast-down [12]–[14]. The EAD strategy considers all four cases and then reduces unreasonable actions. Therefore, it provides the reference speed for vehicles to run in an energy saving manner. However, EAD strategies are only applicable when the vehicle is approaching a signalised intersection rather than running on the entire route. Hence, for vehicles cruising in a speed range, such as driving on the motorway, a control strategy called Pulse and Glide (P&G) operation has been widely studied for internal combustion engine (ICE) vehicles [15], [16]. In ICE vehicles, the engine high efficiency region falls into high loads. Therefore, to improve the engine efficiency and maintain the vehicle's speed within the acceptable speed range, the engine switches on at high loads (vehicle acceleration) region and then switches off (vehicle coastdown) periodically during cruising. Moreover, the P&G operation can be applied to hybrid vehicles to reduce fuel consumption while maintaining the battery state-of-charge [17], [18]. However, in real traffic environments, it is difficult to adjust vehicle speed periodically in this way because the speed will be significantly affected by other road users. Therefore, developing a more flexible speed optimisation of CAVs attracts wide interests in eco-driving investigations.

The developed solutions can be mainly categorised into two types: global optimisation and real-time optimisation. Global optimisation transforms the eco-driving into a global optimisation problem with multiple constraints. The global optimisation optimised vehicle speed for the entire route to achieve the optimal energy efficiency. It is completed offline before vehicle's departure. Both dynamic programming (DP) [19]–[21] and Pontryagin's Minimum Principle (PMP) [22], [23] have been adopted. However, the global optimisation algorithms are based on complete information of the future route and introduce high computational pressure. Real-time traffic information is excluded in these methods so that the optimised results may be selfish and poor against disturbances. Selfish optimisations are based on the ideal assumption that the controlled vehicle is not affected by other traffic participants along the route. Therefore, it is highly possible that the vehicle may not be able to track the reference speed when there is uncertain traffic information. Hence, real-time optimisation based eco-driving strategies are developed considering uncertainties from other vehicles. Ecological adaptive cruise control (eco-ACC) is a typical real-time optimisation based eco-driving strategy, in which model predictive control (MPC) has been widely used. The eco-ACC maintains safe inter-vehicle distances and minimises energy consumption by adapting the vehicle speed in real-time [24]–[28]. CAVs equipped with eco-ACC run in a similar way as the conventional adaptive cruise control (ACC), which follows the preceding vehicle with a desired spacing. The eco-ACC enables more flexible spacing than the conventional ACC, allowing CAVs running at an optimised speed. This guarantees that a higher energy efficiency is achieved and a safe distance is maintained simultaneously. For eco-ACC, the previewed states of other vehicles are provided by V2V [29]–[31] or learning-based predictive models [26]. However, the optimisation result using MPC is impacted by the length of the prediction horizon. A longer prediction horizon improves the optimisation performance but also increases the computational pressure, which makes real-time implementations more challenging. To facilitate the real-time implementation of MPC, the computational burden can be reduced by rationally shortening the prediction horizon [32]. Furthermore, the preview information is limited to a short horizon when using V2V or learning-based predictions. Consequently, the real-time optimisation methods may be suboptimal.

To address this gap, an eco-driving strategy using a two-stage hierarchical control structure that combines global optimisation

(long-term speed optimisation) and real-time optimisation (local adaptation) has been investigated. Before departure, the long-term speed optimisation algorithm optimises vehicle energy efficiency and provides the reference speed using powertrain characteristics and route information. After departure, local adaptation is implemented in real-time that tracks the reference speed and responds to the traffic situation by adjusting the speed. Case studies of combining DP and MPC in the two-stage eco-driving strategy can be found in [33], [34]. Another two-stage hierarchical control strategy that considers the preceding vehicle was designed in [35]. At the first stage, the optimal speed profile is generated through quadratic programming. At the second stage, the local adaptation is adopted to maintain the safe distance between the controlled vehicle and the preceding one. The local adaptation is affected by the speed of the preceding vehicle and therefore, the reference speed is difficult to be tracked. In the above literature, energy consumption was optimised in both stages. However, the optimisation of a single variable on two stages may cause conflicts and lead to no solution.

All the above literature only consider the vehicle longitudinal control rather than lateral control in lane-changing maneuvers. In this work, a less-disturbed eco-driving strategy is designed to minimise the influences from other on-road vehicles. The strategy can also reduce the impact of other vehicles and avoids selfish optimisation, and therefore is more feasible to be implemented in practical transportation systems. In offline planning, the global optimisation strategy based on DP is proposed incorporating the EAD method. The offline planning optimises the CAVs energy consumption at an average traffic speed, so selfish optimisation is prevented. Afterwards, in online tracking, the MPC-based online control is applied to the CAVs. Lateral control is considered in online tracking, while lane-changing and lane-keeping functions are both enabled. The main contributions of this work are stated as follows.

1) The offline planning avoids selfish optimisation. Minimising the speed deviation from the average traffic speed is considered as one of the objectives.
2) Vehicle dynamics are integrated with longitudinal and lateral controls of CAVs in online tracking. Therefore, the lane-changing function is activated to overtake preceding vehicles if necessary. The capability of vehicle overtaking provides greater flexibility in speed tracking than merely following the preceding vehicle in real traffic conditions.
3) The online tracking is freed to focus on path tracking and collision avoidance. Therefore, the design eliminates the conflict of optimisations in both offline planning and online tracking. This guarantees that the proposed method always generates the solution to improve energy efficiency while maintaining the vehicle safety.

The remainder of this paper is structured as follows. The eco-driving strategy is outlined in Section II. The offline planning and online tracking designs are presented in Section III and Section IV. Simulations under the single road segment scenario and real traffic environment are demonstrated and analysed in Section V. Conclusions are made in Section VI.

II. Description of the Less-Disturbed Eco-Driving Strategy

The eco-driving technique is a speed planning method which optimises the vehicle fuel efficiency. In this paper, the investigated vehicle is powered by an ICE.

A. Architecture of the Strategy

The objective of the eco-driving strategy is to continuously improve the fuel efficiency of the CAV in driving. The CAV is assumed to receive traffic light information and the previewed traffic environment information from the SPaT and ITS using V2I. The configuration of the less-disturbed eco-driving strategy is shown in Fig. 1. First, offline planning leads to the optimisation of fuel consumption. Then, the CAV tracks the reference speed using an online tracking algorithm.

Offline planning can produce a fuel efficient reference speed for the controlled CAV based on a global optimisation method. This is realised before the trip starts. The data fusion and speed optimisation are included in offline planning. First, the data fusion merges the previewed traffic information, route map and route plan information to provide the average traffic speed and other information. Then, in speed optimisation, the reference speed is generated from global optimisation based on powertrain characteristics and road conditions. To avoid selfish optimisation, this paper proposes a speed deviation value that is the difference between the speed of the controlled vehicle and the average speed of the current road segment. Each road segment is the trip between two sequential sets of traffic lights. In this paper, the offline planning model is chosen as a distance-based model, because of two reasons. First, the time value is not explicitly available, and hence the DP should be modified to be distance-based, ensuring the satisfaction of time-dependent constraints [25]. Second, in a distance-based driving cycle, any adaptation of the vehicle speed only influences the nearby locations, while the reference speed remains unaffected in other locations [33]. The design details of offline planning are provided in Section III.

During driving, an online tracking strategy is designed to track the reference speed and create trajectory for the CAV. The real-time traffic information including states of other vehicles is considered. Furthermore, the expected states of surrounding vehicles are predicted based on measurements. In this paper, a constant-acceleration model is implemented to predict the vehicles' states [36]. A motion decision making is used to decide the lane-changing or lane-keeping actions for the CAV to minimise the speed deviation, which is based on the real-time traffic information. Furthermore, a local adaptation with multi-objectives based on MPC is proposed to realise speed and lane tracking. Meanwhile, vehicle safety is guaranteed by including collision avoidance constraints in the MPC design. The design details of online tracking are provided in Section IV.

B. Engine Fuel Consumption Model

The engine fuel mass flow rate is described by the engine fuel efficiency map as illustrated in Fig. 2, which is obtained from

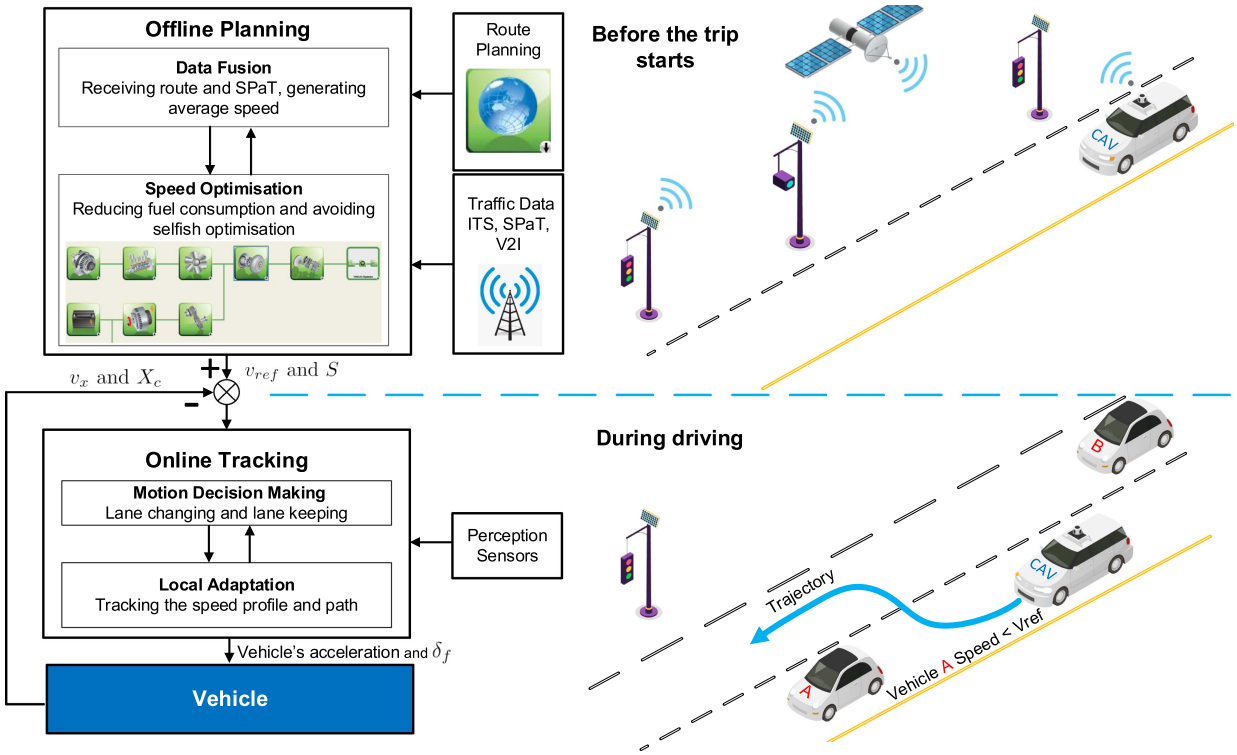

Fig. 1. The architecture of the less-disturbed eco-driving strategy for CAVs.

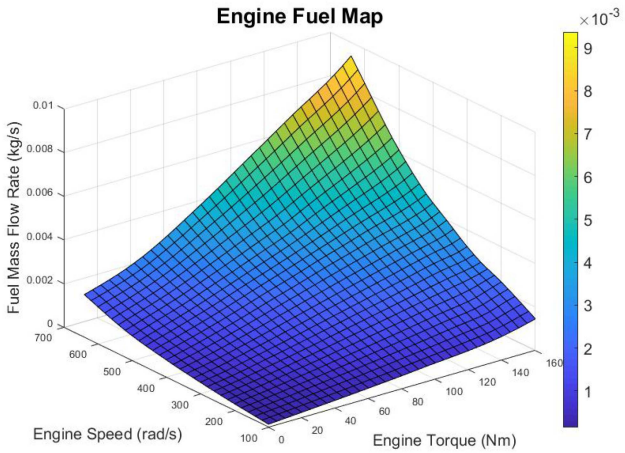

Fig. 2. Engine fuel map extracted from Autonomie.

Autonomie [37]. The engine fuel mass flow rate can be described as

$$\dot{m}_f = f\left(T_\omega, \omega_e\right) \tag{1}$$

where the crankshaft rotational speed can be calculated by

$$\omega_e = r_{\mathrm{gb}}\omega_{\mathrm{wheel}}. \tag{2}$$

C. Vehicle Dynamics

The vehicle dynamics are modeled in two different ways for the offline planning and online tracking. As described earlier, the vehicle dynamics in offline planning are characterised using a distance-based model. Meanwhile, the offline planning excludes the real-time traffic influence, so the model only focuses on longitudinal dynamics. However, the impacts from other vehicles and lane-changing have to be considered in online tracking. Hence, a dynamical bicycle model is employed in online tracking to enable control of the vehicle's longitudinal and lateral movements.

In distance-based offline planning [35], the longitudinal distance step Δs is assumed to be constant. The total route distance S is calculated by

$$S = N\Delta s. \tag{3}$$

The vehicle acceleration is assumed to remain constant within each distance step.

Denote the speed and the driving distance at the location of $k\Delta s$ by $v(k)$ and $S(k)$, respectively. The driving distance at the next location is given by

$$S(k+1) = S(k) + \int_{t_k}^{t_{k+1}} \left(v(k) + a(k)\left(t_{k+1} - t_k\right)\right) \mathrm{d}t \tag{4}$$

where $k \in \{0, 1, \ldots, N-1\}$; t_k and a are the time instant and the acceleration at the location of $k\Delta s$, respectively. Considering the vehicle longitudinal dynamics, the discrete distance-based vehicle dynamics can be described as

$$\begin{aligned} v(k+1) &= v(k) + \frac{a(k)\cdot\Delta s}{v(k)} \\ t(k+1) &= t(k) + \frac{2\cdot\Delta s}{v(k) + \frac{a(k)\cdot\Delta s}{v(k)}} \end{aligned} \tag{5}$$

where $k \in \{0, 1, \ldots, n-1\}$.

The vehicle acceleration is generated by the engine torque, which can be calculated by

$$a(k) = \frac{r_{\mathrm{gb}} T_\omega(k) - T_{\mathrm{brk}}(k)}{m r_w} - g\left(\cos(\theta(k)) C_{\mathrm{rr}} - \sin(\theta(k))\right) - \frac{\rho A C_d}{2\,m} v(k)^2 \quad (6)$$

where the rolling resistance coefficient for all tyres are assumed to be the same.

A dynamical bicycle model describing vehicle longitudinal and lateral dynamics is used in online tracking [38]. The model is described as

$$\begin{aligned}
\dot{v}_x &= v_y \omega_r + a_x \\
\dot{v}_y &= \frac{-2(C_f + C_r)}{m v_x} v_y \\
&\quad - \left[\frac{2(l_f C_f + l_r C_r)}{m v_x} + v_x\right] \omega_r + \frac{2C_f}{m} \delta_f \\
\dot{X}_c &= v_x \cos\psi - v_y \sin\psi \\
\dot{Y}_c &= v_y \cos\psi + v_x \sin\psi \\
\dot{\psi} &= \omega_r \\
\dot{\omega}_r &= \frac{-2(l_f C_f + l_r C_r)}{I_z v_x} v_y \\
&\quad - \frac{2(l_f{}^2 C_f + l_r{}^2 C_r)}{I_z v_x} \omega_r + \frac{2 l_f C_f}{I_z} \delta_f
\end{aligned} \quad (7)$$

where I_z is the moment of inertia of the vehicle about the vertical (z) axis. The front wheel angle δ_f and vehicle longitudinal acceleration a_x are the control inputs.

III. Offline Planning

Offline planning generates a reference speed that aims to minimise fuel consumption and prevent selfish optimisation.

A. Data Fusion

The traffic state information can be measured by fixed sensors such as induction loops and magnetometers. CAV can receive information about the traffic flow rate and traffic density for the future road segments from ITS via V2I. The data fusion method of heterogeneous traffic data has been well developed. A successful fusion algorithm is proposed in [39] to reconstruct traffic states from multiple fixed sensor measurements. In this study, the traffic flow and density are assumed to be known exactly. Subsequently, the average traffic speed for a road segment is calculated by [40]:

$$V^i_{\mathrm{avg}}(k) = \frac{f^i_{\mathrm{flow}}(k)}{f^i_{\mathrm{density}}(k)},\ i = \{1, 2, \ldots, I\} \quad (8)$$

where $f^i_{\mathrm{flow}}(k)$ represents the traffic flow for the i^{th} road segment, which refers to the number of vehicles that pass one point in a given time frame; and $f^i_{\mathrm{density}}(k)$ denotes the traffic density, which is the number of vehicles that occupy the i^{th} road segment at one time.

B. Speed Optimisation

The offline planning generates the reference speed for the controlled CAV based on distance-based vehicle longitudinal dynamics (5). A backward induction DP is applied for vehicle control along the route. The cost function is chosen as

$$J_{\mathrm{opt}} = w_{o,1} \sum_{k \in \{0,1,\ldots,N-1\}} \dot{m}_f(k) + w_{o,2} \sum_{k \in \{0,1,\ldots,N-1\}} \|v(k) - V^i_{\mathrm{avg}}(k)\| \quad (9)$$

where the first term of the cost function represents the fuel consumption and the second term represents the total speed deviation between the vehicle speed $v(k)$ and the average speed of the current road segment. Additionally, $w_{o,1}$ and $w_{o,2}$ indicate the weights of the fuel consumption and speed deviation, respectively. The controlled variables of the CAV are T_ω, T_{brk} and N_{gear}.

Remark 1: The constant average speed $V^i_{\mathrm{avg}}(k)$ for each road segment is used in this study. However, the average speed at each location of the road segment can be variable data to reflect traffic conditions. The average speed has also been used in some other eco-driving methods to optimise vehicle speed, such as [33] and [41]. It is interesting to consider an accurate traffic prediction model to address the problem, such as applying the neural network methods in [42] and [43]. However, most roads only provide limited information on the traffic state under existing conditions, and all traffic models have unexpected disturbances. Meanwhile, the aim of this paper is to demonstrate a new method to optimise the speed to reduce the energy consumption of vehicles taking the same route. Therefore, a predicted average speed of the traffic based on the macroscopic model was used in this study.

The DP has three types of constraints: 1) vehicle constraints concerning physical limits and driving comfort; 2) vehicle speed constraints; and 3) traffic constraints. The physical constraints of the CAV are

$$\begin{aligned}
T^{\min}_\omega \le T_\omega(k) \le T^{\max}_\omega, \forall k \in \{0, 1, \ldots, N\} \\
a^{\min} \le a(k) \le a^{\max}, \forall k \in \{0, 1, \ldots, N\}
\end{aligned} \quad (10)$$

which describe the physical constraints on engine torque and vehicle acceleration, respectively. $T^{\min}_\omega$ and $T^{\max}_\omega$ represent the minimal and maximal allowable engine torque respectively; the maximum acceleration $a^{\max}$ is set as a physically feasible limit in addition to considering passenger comfort, and it is a positive constant; $a^{\min}$ is a negative constant representing the maximum deceleration. The speed constraints in this paper can be categorised into two types: normal speed constraints and final speed constraints. The speed constraints for the last step of each segment $k \in \{l_1, l_2, \ldots, N\}$ are set as final speed constraints. The vehicle queue is discharged when the controlled CAV approaches the intersection. Therefore, the traffic density before the intersection is lower than after the intersection. The

controlled CAV will adjust the speed before approaching the intersection to make driving safer and smoother. The final speed constraints have been set as a velocity range (± 1 m/s) close to the average speed of the next segment. The normal speed constraints are enforced for the rest of the steps. The speed constraints can be written as

$$\begin{cases} v^{\min} \le v(k) \le v^{\max}, \forall k \in \{0, 1, \ldots, N-1\}, \\ \quad \forall k \notin \{l_1, l_2, \ldots, N\} \\ V_{\text{avg}}^{i+1} - 1\,\text{m/s} \le v(k) \le V_{\text{avg}}^{i+1} + 1\,\text{m/s}, \\ \quad \forall k \in \{l_1, l_2, \ldots, N\} \end{cases} \tag{11}$$

which describe the normal speed constraints and final speed constraints, respectively. The maximum velocity $v^{\max}$ is set as the speed limit on the road, and $v^{\min}$ represents the lower-bound speed (i.e. 0 m/s). The EAD based on the SPaT is employed in this paper, while two types of time periods are used. The first one is the vehicle traveling time period, which starts from the vehicle departure, while the other one is the signal cycle time representing the time period of a traffic signal. Each traffic signal cycle time period includes a red phase and a green phase and each cycle starts with the red phase. The time of a CAV passing the intersection can be written as

$$c_p^i = (c_b^i + T_p^i) \bmod c_{\text{period}}^i \tag{12}$$

where $\bmod$ is the modulo operation; c_p^i is the signal cycle time when the vehicle passes the i^{th} intersection; c_b^i is the signal cycle time when the vehicle begins on the route and c_{period}^i is the total length of the traffic signal cycle period at the i^{th} intersection; and the vehicle passing the i^{th} intersection in vehicle traveling time period is represented by T_p^i. Thus, traffic constraints can be written as

$$c_p^i > c_r^i + t_q^i \tag{13}$$

where c_r^i is the red phase time of the traffic light at the i^{th} intersection; and t_q^i denotes the time delay caused by vehicles queuing at the i^{th} intersection. The cost function (9) with vehicle constraints (10), (11) and traffic constraints (13) constitute the speed optimisation. To summarise, the offline planning will create a reference speed v_{ref}, and DP only deals with SPaT information and the average traffic speed rather than real-time traffic conditions.

IV. Online Tracking

After departure, the vehicle is controlled to track the reference speed v_{ref} obtained in offline planning. MPC is adopted to online track the trajectory by solving a constrained optimisation problem. Meanwhile, the online tracking can follow the reference speed using the longitudinal position X_c along the route with the relative distance step Δs.

A. Motion Decision Making

The motion of the preceding vehicle is predicted using a constant-acceleration model [36], which assumes that the object vehicle has a constant acceleration during the prediction horizon. Such model is suitable for short-term predictions. The preceding vehicle motion is predicted using

$$\begin{aligned} v_x^n(p+1) &= v_x^n(p) + T_s \cdot a_m \\ X^n(p+1) &= X^n(p) + T_s \cdot v_x^n(p) \end{aligned} \tag{14}$$

where $p \in \{0, 1, \ldots, P\}$ and T_s is selected as 0.1 s; P is the prediction horizon; and a_m is the acceleration of the preceding vehicle, which is measured at time step $p = 0$. Besides, the preceding vehicle's acceleration is assumed to be constant during the forecast.

Vehicle motion studied in this paper can be categorised into two major types. The first type is that the CAV remains in the current lane and tracks the reference speed when the preceding vehicle does not influence the controlled CAV or there is no vehicle in front. The other type is that the motion decision making will decide the maneuver and path planning for lane changing (if necessary) when the controlled CAV is influenced by the preceding vehicle. In summary, the motions decisions depend on the following four conditions:

- The controlled CAV stays on the same lane of the preceding vehicle

$$l_c = l_n \tag{15}$$

  where l_c and l_n denote the lanes of the controlled CAV and the preceding vehicle, respectively.
- The average longitudinal speed of the controlled CAV is higher than the preceding vehicle during a constant-acceleration prediction period

$$\frac{1}{P}\left(\sum_{p=1}^{P} v_{\text{ref}}(p)\right) > \frac{1}{P}\left(\sum_{p=1}^{P} v_x^n(p)\right). \tag{16}$$

- The distance between the preceding vehicle and the controlled CAV is smaller than the desired distance:

$$d_{\text{safety}_x} + t_s v_x(k) \ge X^n(k) - X_c(k) \tag{17}$$

  where the desired time of motion decision is longer than safety time ($t_s > \delta_{t_x}$).
- To guarantee safety between the surrounding vehicles (vehicles on the target lane) and the controlled CAV, lane-changing is only allowed when the inter-vehicle distance [44] is larger than the safety margin:

$$\mid X_c(k) - X_{l\pm1}(k) \mid \ge \Delta v(k) \cdot t_c + \frac{1}{2} a_{\pm\max}(k) \cdot t_c^2 \tag{18}$$

  where $X_{l\pm1}$ indicates the longitudinal position of the objective vehicle on the target lane ($l \pm 1$); $a_{\pm\max}$ is the maximum acceleration ($X_c > X_{l\pm1}$) or deceleration ($X_c < X_{l\pm1}$) of the objective vehicles; and t_c represents the desired time for lane changing.

In motion decision making, the controller will decide to change lanes only if all the above conditions are satisfied.

B. Local Adaptation

In order to track the speed profile and follow the desired path, the bicycle model (7) is used to represent the CAV's dynamics. The model is discretised using Euler's method with the time step

T_s. The MPC optimisation is formulated as

$$\min\Bigg(w_{r,1}\sum_{k=1}^{N}\|(Y_c(k)-r_y(k)\|^2 + w_{r,2}\sum_{k=1}^{N}\|(v_x(k)-v_{\mathrm{ref}}(k))\|^2\Bigg) \tag{19}$$

subject to:

$$a_x^{\min}\le a_x(k)\le a_x^{\max},\forall k\in\{0,1,\ldots,N_t-1\}$$
$$a_y^{\min}\le a_y(k)\le a_y^{\max},\forall k\in\{0,1,\ldots,N_t-1\}$$
$$v_x^{\min}\le v_x(k)\le v_x^{\max},\forall k\in\{0,1,\ldots,N_t-1\}$$
$$\delta_f^{\min}\le \delta_f(k)\le \delta_f^{\max},\forall k\in\{0,1,\ldots,N_t-1\}$$

where the first term of the cost function (19) represents the lateral deviation and the second term represents the speed tracking error. All of the state variables in the CAV's dynamic model are given in (7). $w_{r,1}$ and $w_{r,2}$ indicate the weights of the lateral position tracking and speed tracking, respectively. The reference lateral position r_y is the centre of the selected lane, which is provided by motion decision making.

Moreover, local adaptation is influenced by other vehicles, so traffic safety restrictions are necessary. In the lane-keeping mode, the CAV should maintain a safe distance with the preceding vehicle, which is to satisfy the following constraint:

$$d_{\mathrm{safety_x}}+\delta_{t_x}\cdot v_x(k)\le X^n(k)-X_c(k). \tag{20}$$

The CAV should also maintain in the current lane, thus the constraints of the CAV lateral position are

$$Y(k)\in\left[\overline{y_l}(k),\ \underline{y_l}(k)\right] \tag{21}$$

where $\overline{y_l}(k)$ and $\underline{y_l}(k)$ are the lateral bounds of the lane l.

In the lane-changing mode, the lateral position constraints are changed to include bounds of both the current lane and the target lane. In addition, motion decision making is utilised to guarantee safety during the maneuver.

V. Simulations

A. Simulations Setup

To validate the performance of the proposed less-disturbed eco-driving strategy, simulations in both single road segment scenario and real traffic environment have been studied. All simulations are conducted via MATLAB and Autonomie. The MPC is modeled and solved using the YALMIP [45] with IPOPT [46] solver. The simulation runs in Matlab R2019a on a computer with an i7-8700 @ 3.20 GHz processor. The average computational time of 1 s real-time tracking on our PC is 0.93 s. The proposed strategy is compared with benchmarks eco-driving strategies and human drivers. The single road segment scenario simulation is based on a long road which allows eco-driving strategy to test lane-changing performance. The real traffic environment simulation is based on a real road setting, and the real human driving tests were conducted on the same road. The results of human driving tests were used as a benchmark to compare with our method. The reference speed provided by offline planning without any disturbances is represented by *Reference*. The selected benchmarks include two eco-driving strategies similar to [47] and [34], which are incapable of lane changing and defined as:

- A two-stage eco-driving strategy with a long-term optimisation and a local adaptation. However, the average traffic speed is not considered in this strategy, which is denoted as *LO only*.
- A two-stage eco-driving strategy with a long-term optimisation and a local adaptation. The speed deviation from the average traffic speed is considered in this strategy, which is denoted as *LO-Vavg*.

All the strategies implemented distance-based speed optimisations to guaranteed that all vehicles finished the trip. Offline planning only considers the average traffic speed rather than traffic density and flow. Although the average speeds are the same, traffic densities and flows may vary. Therefore, two types of scenarios with the same average speed but different traffic densities and flows are discussed:

- The CAV with the proposed strategy that can make lane-changes to track the reference at any time, which is denoted as *Eco 100%*.
- The CAV with the proposed strategy may be unable to execute lane changes due to high traffic densities and flows. As traffic densities and flows increase, the successful rate of lane changing decrease to 60-80%. Therefore, this scenario is denoted as *Eco 60-80%*.

All the simulations are implemented on the same vehicle, whose model is provided by Autonomie. The vehicle is driven by a 2.0 L gasoline engine and equipped with V2V and V2I communications. The analysis for both simulations includes two steps. First, the reference speed provided in offline planning is analysed. Then, the vehicle speed tracking and the fuel consumption are analysed. The values of vehicle parameters are presented as follow: $r_{\mathrm{gb}}=\{17,9.6,6.3,4.6,3.7,3.5\}$, $r_w=0.3\,\mathrm{m}$, $C_d=0.48$, $\theta_g=0^\circ$, $C_{\mathrm{rr}}=0.015$, $m=1800\,\mathrm{kg}$, $A=3\,\mathrm{m}^2$, $l_r=1.015\,\mathrm{m}$, $l_r=1.621\,\mathrm{m}$ and $l=3.5\,\mathrm{m}$.

B. Single Road Segment Scenario

The single road segment scenario simulation is conducted on a 4000 m straight single-direction two-lane carriageway with a signalised intersection at the end of the road. The speed limit of the road is 50 mph (i.e. 22.35 m/s). Meanwhile, the final speed constraints of this road segment has been set as $15\pm1\ \mathrm{m/s}$.

1) Offline Planning: The DP is used to optimise vehicle speed in offline planning. Furthermore, the average traffic speed is calculated by (8) (16 m/s in this driving scenario). In this paper, we assume that the vehicle receives SPaT from intersections before departure via V2I communication. Thus, the EAD strategy is applied in our eco-driving strategy to prevent stopping at the intersection. In this scenario, the results of offline planning are shown in Fig. 3.

The results presented in Fig. 3 are the distance-based reference speed, in which the offline planning of the proposed strategy is represented in blue solid curve, while long-term optimisation

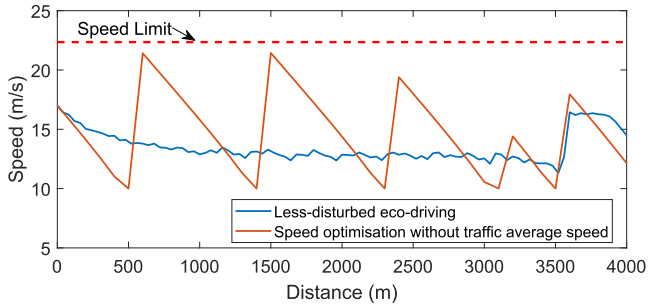

Fig. 3. The speed profiles produced in offline planning, where the average traffic speed is considered (solid blue) or not considered (solid red).

(excluding average traffic speed) is represented by the red solid curve. The results of these two methods present different speed strategies. The offline planning excluding average traffic speed is a typical P&G operation result, in which the vehicle speed is adjusted aggressively and regularly during the cruise. The resulting speed profile has a large difference from the average speed. However, the result of the proposed offline planning strategy is significantly smoother, and the vehicle speed is closer to the average traffic speed.

2) Online Tracking: The online tracking is designed to make the CAV follow the reference speed and cooperate with other vehicles in real-time. The performance of speed tracking influences the CAV energy efficiency. The overtaking maneuver can be achieved via the proposed strategy, which increases vehicle flexibility in tracking the reference speed. However, the CAV cannot guarantee lane-changing, because the final decision depends on the traffic condition.

Fig. 4 show the position and speed of the vehicle controlled by the proposed strategy. The upper subfigure in Fig. 4 shows that the controlled CAV makes lane changes twice during the route as the CAV drives on two-lane carriageway with the width of 3.5 m for each lane. The solid black line is the boundary of the road, and the dashed line represents a broken line dividing the lanes of traffic travelling in the same direction. The vehicle path is represented in red. The lane-changing decision is made by the motion decision making and the path is tracked through local adaptation. The speed tracking is reflected in the lower subfigure of Fig. 4, where the blue dashed curve represents the reference speed provided by the offline planning, and the red curve represents the results of the actual speed. These two curves coincide most of the time, and the only small speed tracking errors are caused due to lane changing.

To compare the speed tracking error with the benchmark driving strategies, a set of the speed error of the proposed strategy, *LO only* and *LO-Vavg* can be seen in Fig. 5. The speed error during the simulation for the *Eco 100%*, *LO-Vavg*, and *LO only* are represented by the blue solid, red dashed, and yellow dotted curves, respectively. In detail, since *LO only* and *LO-Vavg* need to stop at the intersection, their speed tracking errors rise sharply at around 4000 m. The proposed strategy has the best speed tracking performance. Meanwhile, the average Root Mean Square Error (RMSE) of the multi-group proposed strategy, *LO-Vavg* and *LO only* are presented in Fig. 6. The RMSE is calculated by

$$\mathrm{RMSE} = \left[\sum_{i=1}^{N_t}(v_x(i) - v_{\mathrm{ref}}(i))/N_t\right]^{\frac{1}{2}} \tag{22}$$

where N_t is the sample size and equals 4000 in the case study. As shown in Fig. 6, the RMSE of the proposed strategy is 0.293 m/s, while those of *LO-Vavg* and *LO only* are 2.577 m/s and 3.652 m/s, respectively. It can be seen that the RMSE of the proposed strategy is much lower. The preceding vehicle is driving at a varying speed:

$$v_x^n(k+1) = v_x^n(k) + T_s \cdot G(k) \tag{23}$$

where $G(k)$ follows the Gaussian distribution with a mean of 0 and a variance of 1. The initial speed of the preceding vehicle is equal to the average speed. Therefore, the speed error of the benchmark strategies are caused by the preceding vehicle. Subsequently, Fig. 7 reflects the comparison of fuel consumption for the vehicle controlled by the proposed strategy and benchmark strategies, respectively. These results are provided by Autonomie. The results for the vehicle with the proposed strategy (*Eco 100%* or *Eco 60-80%*) has the best fuel consumption compared to the other strategies. Compared with *LO-Vavg* and *LO only*, the proposed strategy (*Eco 100%*) reduced the fuel consumption by 3.1% and 8.7%, respectively.

C. Real Traffic Environment

The driving scenario for the real traffic environment simulation on a real road is shown in Fig. 8, which is a two-lane carriageway with four signalised intersections. The total length of the road is 3450 m, and the speed limit is 50 mph (22.35 m/s). The test vehicle is driving from west to east (left to right), and each part of the road between two intersections has been set as a road segment in the eco-driving strategy. Thus, there are four road segments in the real traffic environment simulation, which are 900 m, 350 m, 1200 m and 1000 m, respectively. Meanwhile, each segment has a different traffic flow rate and density, caused by vehicles joining and leaving the road at the intersections. Therefore, each road segment has a different average speed. During human driving tests, the vehicle has been driven ten times on this test road. There are five times driven by an experienced driver and five times driven by an inexperienced driver. A device is connected to the vehicle via on-board diagnostics to record the vehicle dynamic state and the fuel flow rate of the vehicle. Additionally, by using traffic data and human driving tests, the road simulation model is established in MATLAB to test all the strategies.

1) Offline Planning: To verify the efficiency of the proposed strategy, the speed profile is compared with a human driving speed profile, as shown in Fig. 9. The reference speed provided by the offline planning is shown in red while the speed profile with selected typical human driving characteristics is indicated in blue. As mentioned at the beginning of section V-C, each road segment has a different average speed, and the road segments are connected by the signalised intersections. According to the change of average speed, the speed profile increases stepwisely.

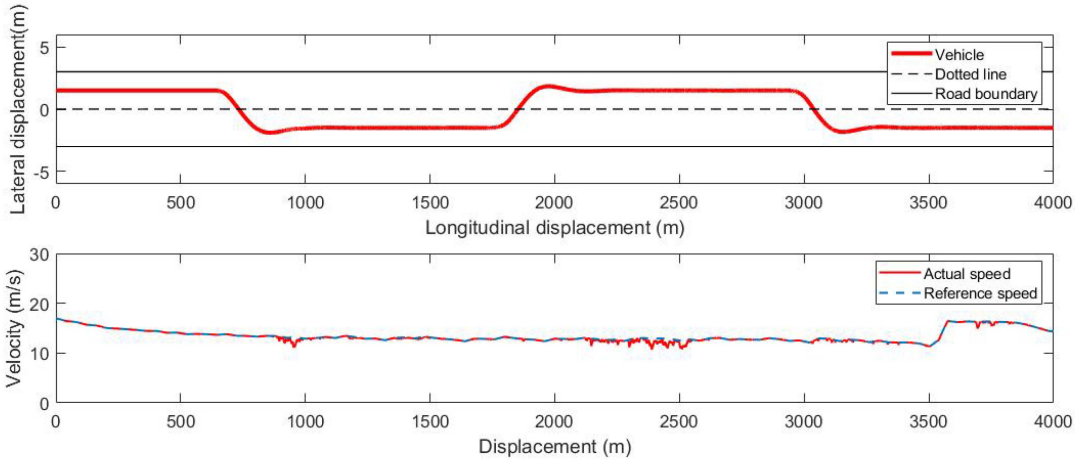

Fig. 4. The position (upper) and speed (lower) of the controlled CAV with the less-disturbed eco-driving strategy.

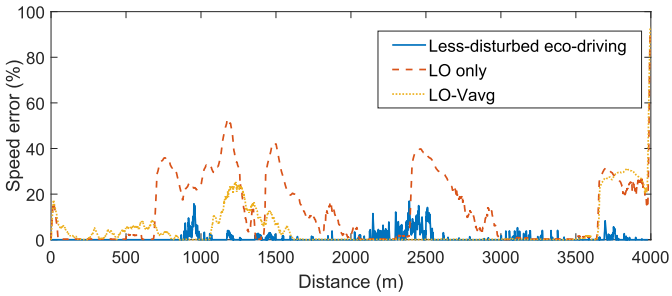

Fig. 5. Speed tracking error during the simulation of less-disturbed eco-driving strategy, *LO-Vavg*, and *LO only*.

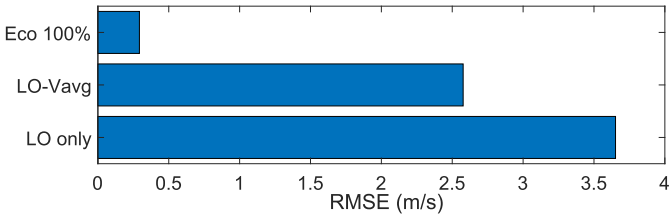

Fig. 6. Root Mean Square Error (RMSE) of tracking error of less-disturbed eco-driving strategy, *LO-Vavg*, and *LO only*.

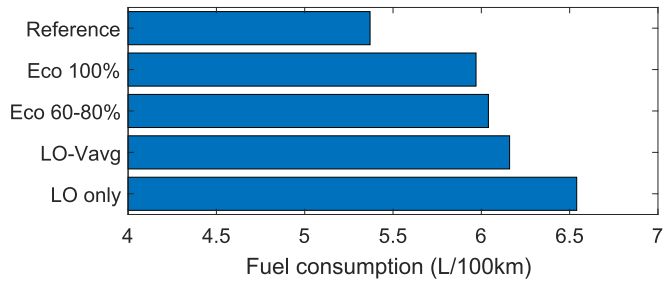

Fig. 7. Fuel consumption of reference speed and all vehicle control strategies.

The average speeds of the sequential road segments are 4 m/s, 7 m/s, 13 m/s and 17 m/s, respectively. The human driven vehicle is stopped at the first and second intersections. Meanwhile, there is a speed fluctuation at about 2400 m, because the driver noticed that the traffic signal is red at the third intersection. However,

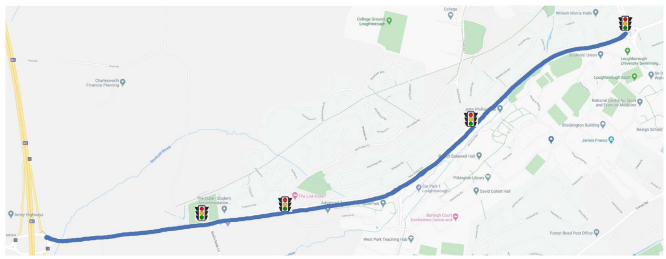

Fig. 8. The real traffic environment. Test road A512, the test vehicle enters the road from M1 junction 23 and leaves at Ashby Road roundabout.

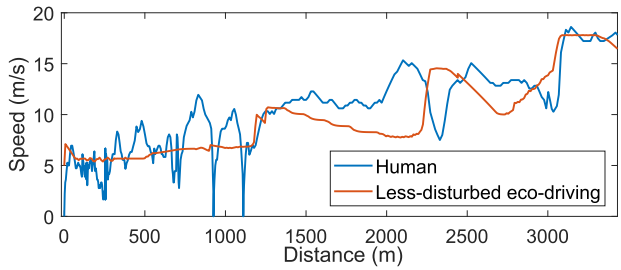

Fig. 9. Speed profile produced in offline planning and a human driver, over the whole route.

the traffic signal turns green when the vehicle decelerates and approaches the intersection.

2) Online Tracking: The online tracking of the proposed strategy has the same configuration as in the single road segment scenario. For the same average traffic speed, the different traffic flow rates and density were designed to reflect the performance of the proposed strategy in different traffic conditions. In order to compare the fuel consumption between vehicles with the proposed strategy, human drivers and other benchmark strategies, a bar graph has been generated, as shown in Fig. 10. The average human driving fuel consumption is denoted by *Human*. Compared with *Human*, the fuel consumption of *Reference* has reduced by 12.2%. However, the controlled CAV is influenced by other vehicles. Therefore, the fuel saving of the proposed strategy is 3.08% for *Eco 60-80%* and 4.53% for *Eco 100%*, as

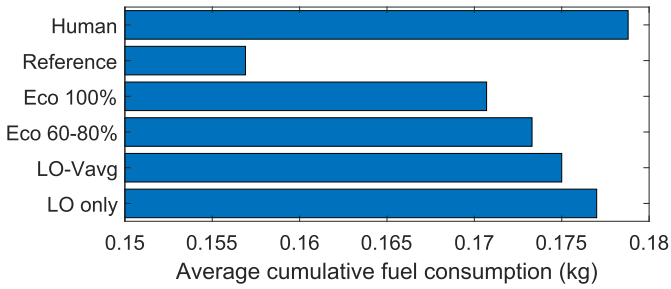

Fig. 10. Average cumulative fuel consumption of human drivers and all strategies.

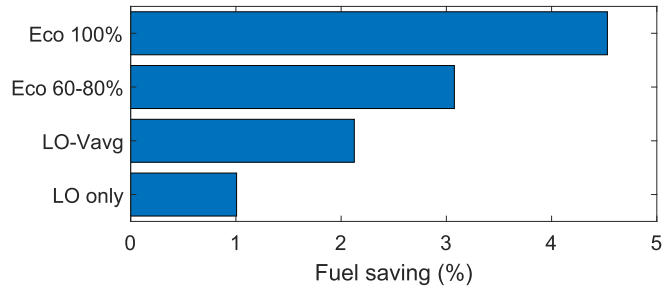

Fig. 11. Percentage of fuel saving for all strategies compared with human drivers.

shown in Fig. 11. Compared with *Human*, the fuel consumption is reduced by 2.13% using *LO-Vavg* and 1.01% using *LO only*. The main reason for the poor performance using benchmark strategies is the big speed tracking errors caused by the need to stop the vehicle at intersections. In both single road segment scenario simulation and real traffic environment simulation, the proposed strategy demonstrated the best fuel efficiency compared to other strategies and human drivers.

VI. Conclusion

The fuel consumption of a vehicle depends on the characteristics of its powertrain, road conditions, and traffic conditions. As there are huge uncertainties regarding future traffic conditions, this paper proposed a less-disturbed eco-driving strategy. The proposed strategy is formed using offline planning and online tracking, which are combined with average traffic speeds and overtaking maneuvers. The consideration of average speed makes the proposed eco-driving strategy have less disturbance to the traffic system. Therefore, it is more feasible to be applied in practical road transportation systems. The lane-changing has minimised the impact from preceding vehicles to maintain the controlled CAV speed in most cases. As a result, the reference speed produced in offline planning has high efficiency for the controlled CAV and at the same time prevents selfish optimisation. Meanwhile, the online tracking with lane-changing capability has the best speed tracking performance. In the selected scenario, the less-disturbed eco-driving strategy can improve the CAV fuel efficiency by 4.53% compared to human drivers. In the future, we will build a reliable traffic prediction model based on model-based and data driven methods, which will further improve safety and reliability. The proposed eco-driving technique will be applied to different powertrain vehicles and also the vehicle platoon.

References

[1] Y. Huang *et al.*, "Eco-driving technology for sustainable road transport: A review," *Renewable Sustain. Energy Rev.*, vol. 93, pp. 596–609, 2018.
[2] M. Zhou *et al.*, "A review of vehicle fuel consumption models to evaluate eco-driving and eco-routing," *Transp. Res. D: Transport Environ.*, vol. 49, pp. 203–218, 2016.
[3] S. Kuutti, S. Fallah, K. Katsaros, M. Dianati, F. Mccullough, and A. Mouzakitis, "A survey of the state-of-the-art localization techniques and their potentials for autonomous vehicle applications," *IEEE Internet Things J.*, vol. 5, no. 2, pp. 829–846, Apr. 2018.
[4] S. W. Loke, "Cooperative automated vehicles: A review of opportunities and challenges in socially intelligent vehicles beyond networking," *IEEE Trans. Intell. Veh.*, vol. 4, no. 4, pp. 509–518, Dec. 2019.
[5] X. Huang and H. Peng, "Speed trajectory planning at signalized intersections using sequential convex optimization," in *Proc. Amer. Control Conf.*, 2017, pp. 2992–2997.
[6] Y. Shao and Z. Sun, "Eco-approach with traffic prediction and experimental validation for connected and autonomous vehicles," *IEEE Trans. Intell. Transp. Syst.*, vol. 22, no. 3, pp. 1562–1572, Mar. 2021.
[7] Z. Wang, G. Wu, and M. J. Barth, "Cooperative eco-driving at signalized intersections in a partially connected and automated vehicle environment," *IEEE Trans. Intell. Transp. Syst.*, vol. 21, no. 5, pp. 2029–2038, May 2020.
[8] Q. Xin *et al.*, "Predictive intelligent driver model for eco-driving using upcoming traffic signal information," *Physica A*, vol. 508, pp. 806–823, 2018.
[9] H. Xia, G. Wu, K. Boriboonsomsin, and M. J. Barth, "Development and evaluation of an enhanced eco-approach traffic signal application for connected vehicles," in *Proc. 16th Int. IEEE Conf. Intell. Transp. Syst.*, 2013, pp. 296–301.
[10] Z. Wei, P. Hao, and M. J. Barth, "Developing an adaptive strategy for connected eco-driving under uncertain traffic condition," in *Proc. IEEE Intell. Veh. Symp.*, 2019, pp. 2066–2071.
[11] G. Mahler, A. Winckler, S. A. Fayazi, M. Filusch, and A. Vahidi, "Cellular communication of traffic signal state to connected vehicles for arterial eco-driving," in *Proc. 20th Int. IEEE Conf. Intell. Transp. Syst.*, 2017, pp. 1–6.
[12] Z. Wang, G. Wu, P. Hao, and M. J. Barth, "Cluster-wise cooperative eco-approach and departure application along signalized arterials," in *Proc. 20th Int. IEEE Conf. Intell. Transp. Syst.*, 2017, pp. 145–150.
[13] O. D. Altan, G. Wu, M. J. Barth, K. Boriboonsomsin, and J. A. Stark, "Glidepath: Eco-friendly automated approach and departure at signalized intersections," *IEEE Trans. Intell. Veh.*, vol. 2, no. 4, pp. 266–277, Dec. 2017.
[14] X. Qi, G. Wu, P. Hao, K. Boriboonsomsin, and M. J. Barth, "Integrated-connected eco-driving system for phevs with co-optimization of vehicle dynamics and powertrain operations," *IEEE Trans. Intell. Veh.*, vol. 2, no. 1, pp. 2–13, Mar. 2017.
[15] S. E. Li and H. Peng, "Strategies to minimize the fuel consumption of passenger cars during car-following scenarios," *Proc. Inst. Mech. Eng., Part D: J. Automobile Eng.*, vol. 226, no. 3, pp. 419–429, 2012.
[16] J. O. Han, "Fundamentals of energy efficient driving for combustion engine and electric vehicles: An optimal control perspective," *Automatica*, vol. 103, pp. 558–572, 2019.
[17] Z. Pan, S. Shieh, and B. Li, "Battery state-of-charge pulse-and-glide strategy development of hybrid electric vehicles for VTS motor vehicle challenge," in *Proc. IEEE Veh. Power Propulsion Conf.*, 2018, pp. 1–7.
[18] S. Shieh, T. Ersal, and H. Peng, "Pulse-and-glide operation for parallel hybrid electric vehicles with step-gear transmission in automated car-following scenario with ride comfort consideration," in *Proc. Amer. Control Conf.*, 2019, pp. 959–964.
[19] C. Sun, X. Shen, and S. Moura, "Robust optimal eco-driving control with uncertain traffic signal timing," in *Proc. Amer. Control Conf.*, 2018, pp. 5548–5553.
[20] E. Ozatay *et al.*, "Analytical solution to the minimum energy consumption based velocity profile optimization problem with variable road grade," *IFAC Proc. Volumes*, vol. 47, no. 3, pp. 7541–7546, 2014.
[21] E. Ozatay *et al.*, "Cloud-based velocity profile optimization for everyday driving: A dynamic-programming-based solution," *IEEE Trans. Intell. Transp. Syst.*, vol. 15, no. 6, pp. 2491–2505, Dec. 2014.

[22] E. Ozatay *et al.*, "Velocity profile optimization of on road vehicles: Pontryagin's maximum principle based approach," *Control Eng. Pract.*, vol. 61, pp. 244–254, 2017.
[23] D. Shen, D. Karbowski, and A. Rousseau, "A minimum principle-based algorithm for energy-efficient eco-driving of electric vehicles in various traffic and road conditions," *IEEE Trans. Intell. Veh.*, vol. 5, no. 4, pp. 725–737, Dec. 2020.
[24] B. Asadi and A. Vahidi, "Predictive cruise control: Utilizing upcoming traffic signal information for improving fuel economy and reducing trip time," *IEEE Trans. Control Syst. Technol.*, vol. 19, no. 3, pp. 707–714, May 2011.
[25] S. G. Dehkordi *et al.*, "Ecological and safe driving: A model predictive control approach considering spatial and temporal constraints," *Transp. Res. Part D: Transport Environ.*, vol. 67, pp. 208–222, 2019.
[26] D. Moser, R. Schmied, H. Waschl, and L. del Re, "Flexible spacing adaptive cruise control using stochastic model predictive control," *IEEE Trans. Control Syst. Technol.*, vol. 26, no. 1, pp. 114–127, Jan. 2018.
[27] J. Han, A. Sciarretta, L. L. Ojeda, G. De Nunzio, and L. Thibault, "Safe-and eco-driving control for connected and automated electric vehicles using analytical state-constrained optimal solution," *IEEE Trans. Intell. Veh.*, vol. 3, no. 2, pp. 163–172, Jun. 2018.
[28] X. Lin *et al.*, "Simplified energy-efficient adaptive cruise control based on model predictive control," *IFAC-PapersOnLine*, vol. 50, no. 1, pp. 4794–4799, 2017.
[29] X. Hu, H. Wang, and X. Tang, "Cyber-physical control for energy-saving vehicle following with connectivity," *IEEE Trans. Ind. Electron.*, vol. 64, no. 11, pp. 8578–8587, Nov. 2017.
[30] B. Sakhdari and N. L. Azad, "A distributed reference governor approach to ecological cooperative adaptive cruise control," *IEEE Trans. Intell. Transp. Syst.*, vol. 19, no. 5, pp. 1496–1507, May 2018.
[31] H. Yang, H. Rakha, and M. V. Ala, "Eco-cooperative adaptive cruise control at signalized intersections considering queue effects," *IEEE Trans. Intell. Transp. Syst.*, vol. 18, no. 6, pp. 1575–1585, Jun. 2017.
[32] J. L. Garriga and M. Soroush, "Model predictive control tuning methods: A review," *Ind. Eng. Chem. Res.*, vol. 49, no. 8, pp. 3505–3515, 2010.
[33] H. Lim, C. C. Mi, and W. Su, "A distance-based two-stage ecological driving system using an estimation of distribution algorithm and model predictive control," *IEEE Trans. Veh. Technol.*, vol. 66, no. 8, pp. 6663–6675, Aug. 2017.
[34] S. O. Bae, "Design and implementation of ecological adaptive cruise control for autonomous driving with communication to traffic lights," in *Proc. Amer. Control Conf.*, 2019, pp. 4628–4634.
[35] H. Lim, W. Su, and C. C. Mi, "Distance-based ecological driving scheme using a two-stage hierarchy for long-term optimization and short-term adaptation," *IEEE Trans. Veh. Technol.*, vol. 66, no. 3, pp. 1940–1949, Mar. 2017.
[36] M. Brannstrom, E. Coelingh, and J. Sjöberg, "Model-based threat assessment for avoiding arbitrary vehicle collisions," *IEEE Trans. Intell. Transp. Syst.*, vol. 11, no. 3, pp. 658–669, Sep. 2010.
[37] S. Pagerit *et al.*, "Complex system engineering simulation through co-simulation," *SAE Tech. Paper*, Tech. Rep. 2014-01-1106, 2014, doi: 10.4271/2014-01-1106.
[38] R. Rajamani, *Vehicle Dynamics and Control*. Berlin/Heidelberg, Germany: Springer Science & Business Media, 2011.
[39] E. Lovisari *et al.*, "Density/flow reconstruction via heterogeneous sources and optimal sensor placement in road networks," *Transp. Res. Part C. Emerg. Technol.*, vol. 69, pp. 451–476, 2016.
[40] R. A. Anand, L. Vanajakshi, and S. C. Subramanian, "Traffic density estimation under heterogeneous traffic conditions using data fusion," in *Proc. IEEE Intell. Veh. Symp.*, 2011, pp. 31–36.
[41] K. Huang, X. Yang, Y. Lu, C. C. Mi, and P. Kondlapudi, "Ecological driving system for connected/automated vehicles using a two-stage control hierarchy," *IEEE Trans. Intell. Transp. Syst.*, vol. 19, no. 7, pp. 2373–2384, Jul. 2018.
[42] J. Tang, F. Liu, Y. Zou, W. Zhang, and Y. Wang, "An improved fuzzy neural network for traffic speed prediction considering periodic characteristic," *IEEE Trans. Intell. Transp. Syst.*, vol. 18, no. 9, pp. 2340–2350, Sep. 2017.
[43] X. Ma *et al.*, "Long short-term memory neural network for traffic speed prediction using remote microwave sensor data," *Transp. Res. Part C Emerg. Technol.*, vol. 54, pp. 187–197, 2015.
[44] Y. Zhong, L. Guo, Y. Zhang, Q. Liu, and H. Chen, "Optimal lane change control of intelligent vehicle based on MPC," in *Proc. Chin. Control Decis. Conf.*, 2019, pp. 1468–1473.
[45] J. Löfberg, "YALMIP: A toolbox for modeling and optimization in MATLAB," *Proc. IEEE Int. Conf. Robot. Automat.*, vol. 3, pp. 284–289, 2004.
[46] A. Wächter and L. Biegler, "On the implementation of an interior-point filter line-search algorithm for large-scale nonlinear programming," *Math. Prog.*, vol. 106, pp. 25–57, 2006.
[47] G. Obereigner, P. Polterauer, and L. del Re, "A two-layer approach for ecodriving under traffic," in *Proc. Amer. Control Conf.*, 2020, pp. 2282–2287.

Jinsong Yang received the B.E. degree in automotive engineering from the University of Huddersfield, Huddersfield, U.K., and the M.S. degree in automotive engineering from Loughborough University, Loughborough, U.K., in 2017 and 2018, respectively. He is currently working toward the Ph.D. degree with the University of Glasgow, Glasgow, U.K. His current research interests include connected and automated vehicles and energy-saving intelligent vehicles.

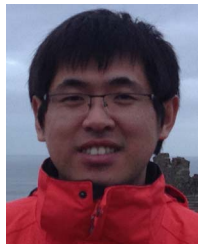

Dezong Zhao (Senior Member, IEEE) received the B.Eng. and M.S. degrees in control science and engineering from Shandong University, Jinan, China, in 2003 and 2006, respectively, and the Ph.D. degree in control science and engineering from Tsinghua University, Beijing, China, in 2010. Since 2020, he has been a Senior Lecturer of autonomous systems with the University of Glasgow, Glasgow, U.K. His research interests include connected and autonomous vehicles, machine learning, and control engineering.

Jingjing Jiang (Member, IEEE) received the B.E. degree from the University of Birmingham, Birmingham, U.K., in 2010, the M.S. degree in control systems from Imperial College London, U.K., in 2011, and the Ph.D. degree in control engineering from Imperial College London, in 2016. She is currently a Lecturer of intelligent mobility and autonomous vehicles with Loughborough University, Loughborough, U.K. Her research interests include autonomous vehicles, advanced driving assistance system design, and human-machine interactions.

Jianglin Lan received the B.E. degree from South China Agricultural University, Guangzhou, China, the M.S. degree from the South China University of Technology, Guangzhou, China, and the Ph.D. degree from the University of Hull, Hull, U.K., in 2011, 2014, and 2017, respectively. He is currently a Research Associate with Imperial College London, London, U.K., and was a Research Associate with the University of Glasgow, Glasgow, U.K., Loughborough University, Loughborough, U.K., and The University of Sheffield, Sheffield, U.K. His research interests include machine learning, optimization, and control for dynamic systems.

Byron Mason received the B.E. degree in mechanical engineering and the Ph.D. degree in powertrain calibration and control from the University of Bradford, Bradford, U.K., in 2005 and 2009, respectively. From 2007 to 2015, he was a Lecturer, then a Senior Lecturer of mechanical engineering with the University of Bradford. He is currently a Senior Lecturer of intelligent powertrain systems with the Department of Aeronautical and Automotive Engineering, Loughborough University, Loughborough, U.K.

Daxin Tian (Senior Member, IEEE) is currently a Professor with the School of Transportation Science and Engineering, Beihang University, Beijing, China. His current research interests include mobile computing, intelligent transportation systems, vehicular ad hoc networks, and swarm intelligent. He is an IEEE Intelligent Transportation Systems Society Member and IEEE Vehicular Technology Society Member.

Liang Li (Senior Member, IEEE) received the Ph.D. degree in mechanical engineering from the Department of Automotive Engineering, Tsinghua University, Beijing, China, in 2008. Since 2017, he has been a Tenured Professor with Tsinghua University. His research interests mainly include vehicle dynamics and control, adaptive and nonlinear system control, and hybrid vehicle develop and control.